Journal of Equine Veterinary Science 104 (2021) 103704

Contents lists available at ScienceDirect

Journal of Equine Veterinary Science

journal homepage: www.j-evs.com

Contrast Enhanced Computed Tomography Findings in 105 Horse Distal Extremities

Frederik Pauwels[a,*], Angela Hartmann[a], John Alawneh[b], Paul Wightman[a], Jimmy Saunders[c]

[a] Radiology Department, Massey University School of Veterinary Science, University Ave, Palmerston North, New Zealand
[b] Murdoch University, School of Veterinary Medicine, Murdoch 6150, Western Australia, Australia
[c] Radiology Department, School of Veterinary Medicine, University of Gent, Merelbeke, Belgium

ARTICLE INFO

Article history:
Received 15 December 2020
Received in revised form 30 June 2021
Accepted 6 July 2021
Available online 10 July 2021

Key words:
Horse
Computed tomography
Arteriography
Arthrography
Bursography

ABSTRACT

The poor soft tissue conspicuity of CT can be improved by using intra-arterial CT Angiography (CTA), and intra-articular and intra-bursal contrast enhanced CT (CTAR). This retrospective study describes a combination protocol of CT and CTA of the horse's foot, and CTAR of the distal interphalangeal joint and navicular bursa. It is hypothesized this would provide a comprehensive overview of the range and severity of distal limb pathology. Radiology reports of all horses admitted for distal limb CT over a 5 year period were reviewed. All horses with a complete four stage CT examination and radiology report with lameness isolated to the foot were included. Twenty seven imaging findings using a four grade semi-quantitative severity scoring system contributing towards six main diagnostic categories were described. One hundred and five examinations on 56 horses revealed a diagnosis of navicular bone disease in 64%, deep digital flexor tendinopathy in 43%, distal interphalangeal osteoarthritis in 35%, navicular bursitis in 31%, distal interphalangeal collateral ligament desmopathy in 26%, and hoof capsule and distal phalanx pathology in 10%. Only 25% of the navicular bone disease cases were considered clinically significant. The majority of deep digital flexor tendon lesions (77%) and distal interphalangeal joint osteoarthritis (51%) were considered significant. Approximately one third of navicular bursa (37%) and collateral ligament (33%) abnormalities were considered significant. Navicular bursa abnormalities were associated with navicular bone and deep digital flexor tendon lesions. The findings support the hypothesis and the use of this protocol for evaluation of foot lameness.

1. Introduction

Cross sectional imaging, both MRI and CT, for the examination of lameness isolated to the horse's foot, performed under standing sedation or general anesthesia has become widely used in referral settings[1]. MRI is accepted as the gold standard for soft tissue imaging, whereas the spatial resolution of CT delivers better bony detail [2].

The relatively poor soft tissue conspicuity of CT [3] has been offset somewhat by the use of Contrast Enhanced CT techniques (CECT). The techniques of intra-arterial CT Angiography (CTA), intra-articular and intra-bursal CT Arthrography (CTAR) for lameness diagnosis have been described [4–6]. The conspicuity of soft tissue lesions is increased due to vascular dilation and neovascularization, or absence of enhancement due to necrosis with CTA[7]. The visualization of cartilage surfaces, intra- or peri-articular ligaments, synovial proliferation and adhesion formation is increased using CTAR [8,9].

The results of a combined examination protocol of standard bone and soft tissue algorithm CT of the horses's foot, CTA of the foot and CTAR of the distal interphalangeal joint and navicular bursa have not been published yet. Clinical decision making after advanced imaging is most often based on the radiology report. In this descriptive retrospective review of radiology reports, we report on the results of 105 foot examinations using this combination protocol. We hypothesized this combination protocol would provide a comprehensive overview of distal limb pathology and provide a useful comparison with results from MRI examinations.

Ethical Statement: The research and manuscript is entirely based on retrospective analysis of medical records. The horses admitted to the veterinary teaching hospital undersign an admission form allowing the use of the medical information for retrospective research evaluation and teaching. Separate ethics committee approval for this retrospective descriptive study was therefore not sought.

* Corresponding author at Frederik Pauwels DVM, CertVA, DipACVS, DipECVDI(LA) . Plexus Veterinary Consulting, Wainui, 4010 Gisborne, New Zealand
E-mail address: fred@plexusveterinaryimaging.com (F. Pauwels).

https://doi.org/10.1016/j.jevs.2021.103704

2. Materials and Methods

Radiology reports and discharge instructions of all horses admitted to the Massey University Teaching hospital for distal limb CT from April 2011 to November 2016 were analyzed. Inclusion criteria were horses (1) in which forelimb lameness had been isolated distal to the fetlock by either a palmar digital nerve block or abaxial nerve block and (2) of which all four of the CT examination techniques described below had been completed and (3) for which a full imaging report and discharge instructions were available. Horses which were referred for CT as a pre-operative planning tool such as keratoma removal, and horses which had an abaxial nerve block performed and had positive imaging findings in the included metacarpophalangeal region were excluded. The selection was performed by an ACVS boarded equine surgeon. The source population are horses in the referral catchment, the study population are the eligible horses, and the study unit of analysis is the imaging finding of the foot, the foot being defined as the structures distal to the proximal interphalangeal joint of the horse.

Horses were unilaterally or bilaterally lame as per the referring veterinarian. Repeat clinical examination was variably performed, including perineural analgesia depending on whether the horse was referred as an imaging outpatient or clinical referral.

The owners of the horses admitted to the veterinary teaching hospital undersign an admission form allowing the use of the medical information for retrospective research evaluation and teaching. Separate ethics committee approval for this retrospective descriptive study was therefore not sought.

The standard four-stage CT protocol included: (1) a distal limb bone and soft tissue algorithm CT acquisition, (2) a distal limb CT arteriogram, (3) a distal interphalangeal CT arthrogram, and (4) a navicular CT bursogram. This protocol was executed under general anesthesia with horses placed in lateral recumbency on a propose built equine CT table (Brilliance CT Equine table, Philips Brilliance, Philips Healthware NV, Eindhoven, The Netherlands) with the to be examined limb dependant, using a 16 slice standard bore multidetector CT unit (Philips Brilliance, Philips Healthware NV, Eindhoven, The Netherlands) in helical mode with slice thickness of 0.6 mm, pitch of 0.438, slice increment of 0.4 mm, tube rotation time 0.75 sec, 401 mAs/slice and kVp of 120 using a high resolution filter. The image FOV was 158 mm and matrix dimensions were 768×768. The protocol was performed bilaterally as standard, with exception of few cases. For this, the horse was moved into the other lateral position and the four-stage protocol repeated.

For the native series (1), the images were acquired from the proximal aspect of the proximal sesamoid bones to the tip of the hoof and reconstructed into 0.6 mm slice thickness in a bone and soft tissue algorithm. For (2) a CT contrast arteriogram of the same region was performed and reconstructed in the same manner. The arteriogram protocol uses a 20G catheter placed in the radial artery proximal to the carpal retinaculum under ultrasound guidance. Flow rates were 2 mL/sec of 150 mgL/mL Iohexol (Omnipaque GE Healthcare Australia PTY Ltd 32 Phillip St Parramatta NSW 2150, GE Healthcare Limited Auckland NZ) (50% diluted 300 mgL/mL Iohexol in saline) from a pressure injector (Medrad Vistron CT injection system model no. VHU600, One Medron Drive, Indianola, PA, 1501, USA) following a previously described protocol [3,4,10]. The acquisition was started 8 seconds after start of injection over the same region with the same settings as the initial acquisition. For (3), the distal interphalangeal joint was injected using a dorsal approach parallel to the solar surface of the foot [11] using a 20G needle and 30 ml of 150 mgL/mL Iohexol (Omnipaque GE Healthcare Australia PTY Ltd 32 Phillip St Parramatta NSW 2150, GE Healthcare Limited Auckland NZ). A portion of the 30 mL of contrast agent was used to inject the joint to palpable distention. An acquisition was performed as described above, starting approximately from the mid diaphysis of the second phalanx and reconstructed in a 0.6 mm slice thickness bone algorithm. For (4), the navicular bursa was injected using a palmar midline approach using a 20G 2.5 inch spinal needle[11] and the bursa injected to distention with 150 mgL/mL Iohexol (Omnipaque GE Healthcare Australia PTY Ltd 32 Phillip St Parramatta NSW 2150, GE Healthcare Limited Auckland NZ). The needle placement was verified prior to injection using a scout CT image. The same CT acquisition and reconstruction as for (3) was performed. Near the end of the review period, (3) and (4) were sometimes combined in one acquisition.

The combined 4 CT examinations per limb were reviewed on a designated CT workstation (Extended Brilliance Workspace running on windows XP software version, Phillips Medical Systems PO Box 10 000, 5680 DA BEST, The Netherlands), or using a viewing software capable of multiplanar reconstruction (eFilm Workstation 3.2, Merge Healthcare, Chicago, IL, USA; Osirix imaging software, Pixmeo, Geneva, Switzerland), where window level and width could be adjusted at will. Imaging reports were written and reviewed by either a ACVR-board certified radiologist (AH) or ACVS-board certified equine surgeon in ECVDI large animal imaging residency training (FP).

Population variables recorded were date of examination, age, sex, horse type, limb examined, lameness grade (AAEP), site positive to nerve blocking, lameness duration (weeks). A four grade semiquantitative severity scoring system of each individual imaging finding in the report was developed. Grade 0 is normal. Grade 1 is a mildly abnormal finding, but not of that severity that it would be by itself be considered clinically significant. Grade 2 is moderately abnormal, considered likely to be causing clinical disease or pain. Grade 3 is very abnormal/severe, almost certainly causing clinical disease. If an imaging finding was not mentioned in the report, it was recorded as normal. These different imaging findings and their severity score contribute towards the imaging diagnoses and their severity score. Diagnostic grade 0 is not present or mentioned. Grade 1 diagnosis equates to an imaging diagnosis which may or may not be clinically significant. Grade 2 diagnosis is most likely clinically significant. Grade 3 diagnosis is no doubt clinically significant. Twenty seven imaging variables in total contributing to the different diagnostic categories were graded. In addition, for lesions within the deep digital flexor tendon, size increase, localization in zones (at the level of the proximal interphalangeal joint, proximal to the navicular bone, at the level of the navicular bone and distal to the navicular bone), and contrast enhancement of the lesions was recorded (central, peripheral to a hypoattenuating region, focal or diffuse) as described in a previous publication [10]. The imaging findings and diagnostic categories are described inTable 1.

The individually graded imaging findings were combined into six main diagnostic categories: navicular bone disease, deep digital flexor tendinopathy, distal interphalangeal joint osteoarthritis, navicular bursitis, distal interphalangeal joint collateral ligament desmopathy, and hoof capsule and distal phalanx pathology. These diagnostic categories were graded 2 fold: once based on severity of imaging findings only from the findings section of the radiology report independently from the conclusion and recommendations sections, and once with a subjective weighting applied, this by taking in account the conclusion section and recommendations of the imaging report and discharge instructions.

First order descriptive statistics were generated for diagnostic grading and diagnostic grading weighted by conclusion and recommendation sections. The homogeneity of grades derived from diagnostic grading and grading weighted by conclusion and recommendation sections were compared using Mann-Whitney-Wilcoxon Test for independence. Statistical significance was declared at an alpha of 0.05 or greater. Statistical analysis was conducted in R (R Core Development Team, 2019). The data organization, statis-

Table 1
Frequency distribution (percentages) of imaging examination (n = 105) severity (grade 0-3) stratified by anatomical structure.

		Grade [n (%)]			
Imaging Diagnosis	Imaging Finding	0	1	2	3
Navicular Bone Disease		38 (36)	49 (47)	17 (16)	1 (1)
	Facies flexoria remodelling	100 (95)	3 (3)	2 (2)	0 (0)
	Facies flexoria cartilage erosion or adhesion	99 (94)	2 (2)	3 (3)	1 (1)
	Facies articularis osteophyte	102 (97)	2 (2)	1 (1)	0 (0)
	CSL insertional remodelling	92 (88)	8 (8)	4 (4)	1 (1)
	Distal border fragmentation	82 (78)	15 (14)	8 (8)	0 (0)
	Medullary sclerosis	100 (95)	2 (2)	2 (2)	1 (1)
	Synovial invagination abnormalities	47 (45)	43 (41)	15 (14)	0 (0)
	Central cyst formation	101 (96)	2 (2)	1 (1)	1 (1)
	Impar ligament abnormalities	94 (90)	7 (7)	3 (3)	1 (1)
	CSL desmitis	102 (97)	0 (0)	3 (3)	0 (0)
Navicular Bursitis		73 (70)	20 (19)	10 (10)	2 (2)
	Adhesion	98 (93)	1 (1)	4 (4)	2 (2)
	Distention	75 (71)	20 (19)	8 (8)	2 (2)
	Synovial Contrast enhancement	91 (87)	6 (6)	6 (6)	2 (2)
Deep Digital Flexor Tendinopathy		61 (58)	9 (8)	28 (27)	7 (7)
DDFT - core lesion		64 (61)	9 (9)	27 (26)	5 (5)
DDFT - split		103 (98)	0 (0)	1 (1)	1 (1)
DDFT - dorsal border lesion		78 (74)	0 (0)	16 (15)	11 (10)
DIPJ Osteoarthritis		68 (65)	17 (16)	17 (16)	3 (3)
	Synovial proliferation, joint distention or adhesions	90 (86)	10 (10)	4 (4)	1 (1)
	Synovial contrast enhancement	92 (88)	3 (3)	5 (5)	5 (5)
	DIPJ osteophyte formation	90 (86)	8 (8)	6 (6)	1 (1)
	DIPJ narrowing	100 (95)	5 (5)	0 (0)	0 (0)
	Arthrogram cartilage defects	84 (80)	7 (7)	10 (10)	4 (4)
	Subchondral bone sclerosis, erosion or cyst formation	102 (97)	0 (0)	1 (1)	2 (2)
DIPJ Collateral Ligament Desmopathy		78 (74)	18 (17)	7 (7)	2 (2)
	Collateral ligament contrast enhancement	89 (85)	10 (10)	4 (4)	2 (2)
	Collateral ligament enlargement	97 (92)	3 (3)	5 (5)	0 (0)
	Collateral ligament origin remodeling	101 (96)	4 (4)	0 (0)	0 (0)
	Collateral ligament insertion remodeling	92 (88)	7 (7)	3 (3)	3 (3)
Hoof Capsule and Distal Phalanx Pathology		99 (94)	4 (4)	2 (2)	0 (0)
	Abnormal laminar contrast enhancement	99 (94)	5 (5)	1 (1)	0 (0)
Keratoma		98 (93)	2 (2)	3 (3)	2 (2)
Pedal osteitis		101 (96)	2 (2)	2 (2)	0 (0)

Table 1: Grade 0: Normal. Grade 1: Mildly abnormal finding or diagnosis, which may or may not be clinically significant. Grade 2: Moderately abnormal finding or diagnosis, considered likely to be causing clinical disease or pain. Grade 3: Severely abnormal finding or diagnosis, almost certainly causing clinical disease or pain. If an imaging finding was not mentioned in the report, it was recorded as a grade 0.

tical test selection and completion was performed by a boarded epidemiologist (JA).

3. Results

There were 105 examinations conducted on 56 horses that fitted the inclusion criteria. Of these horses, seven had unilateral and 49 had bilateral examinations. *Forty-nine per cent* of all examinations involved the left foot and 51% the right foot. There were 38 geldings and 18 mares. Of these, 25 were sport horses (Thoroughbred cross or warmblood), 15 Thoroughbreds, 16 others (7 station bred, 4 warmblood cross, 1 quarter horse, 1 standardbred, 1 pony, 2 not recorded). The average age was 9 years old (Interquartile range [IQR] = 7–11). Forty-eight horses were bilaterally lame, seven unilaterally lame, and one was not reported as to uni- or bilaterally lame. The average lameness grade was 2of 5 (AAEP, IQR 1–2) and the average duration of lameness 8 weeks (IQR 0–25).

In 95 of the 105 distal extremity examinations (91%), more than one diagnosis was made. Of these 95 examinations, 61 had one or more than one diagnosis with a grade > 1 (64%). In 30 examinations, one diagnosis with a grade of > 1 was observed. In 24 examinations, two lesions with a grade > 1 were observed. In seven examinations, three or more lesions with a grade > 1 were observed. Twelve of the 105 examinations (11%) showed no lesions.

3.1. Overall diagnostic categories

An overview of all diagnoses subcategorized in grade with their respective contributing imaging findings is available in Table 1 and supp. Fig 1. A diagnosis of navicular bone disease was made in 64% (n=67), deep digital flexor tendinopathy in 43% (n=44), distal interphalangeal osteoarthritis in 35% (n=37), navicular bursitis in 31% (n=32), distal interphalangeal collateral ligament desmopathy in 26% (n=27), and hoof capsule and distal phalanx pathology in 10% (n=11).

3.2. Navicular bone disease

Of the 67 extremities diagnosed with navicular bone disease (64%), 49 were a grade 1, 17 grade 2 and 1 grade 3 (18 combined over grade 1). The most frequent imaging finding for all grades combined were enlarged synovial invaginations (n=58) and distal border fragments (n =23) (supp. Fig 2). Facies flexoria remodelling and cartilage erosions or adhesion formation was present in six horses, four of which had deep digital flexor tendon lesions. Distal sesamoidean (impar) ligament desmopathy and collateral sesamoidean ligament desmopathy was diagnosed in 11 and three extremities with navicular bone disease respectively.

3.2. Deep digital flexor tendinopathy

Of the 44 extremities diagnosed with deep digital flexor tendinopathy (43%) (Fig. 1), 9 were grade 1, 28 grade 2 and 7 grade 3. The most frequent deep digital flexor tendinopathy diagnoses were deep digital flexor tendon (DDFT) core lesion (n=9) in grade 1, DDFT core lesion (n=27) and dorsal border lesion (n = 16) in grade 2, and DDFT core lesion (n=5) and dorsal border lesion (n=11) in grade 3. There were few tendon splits visualized (n=2) (supp. Fig 3). Diffuse lobar tendon enlargement was present in 13

Fig. 1. Transverse multiplanar reconstruction arteriogram at the suprasesamoidean level: Lateral is left in the image. Severe distention of the navicular bursa and synovial contrast enhancement is present. Enlargement of the medial lobe of the deep digital flexor tendon, and severely increased dorsal vascular contrast enhancement of the dorsal aspect of the medial lobe is present. A linear region of hypoattenuation with surrounding vascular enhancement is consistent with a tendon split (BLACK ARROWHEAD). There is connecting soft tissue between the dorsal aspect of the medial lobe and the dorsal bursa synovium consistent with adhesion formation (WHITE ARROWHEAD).

of the 44 tendinopathy cases. Contrast enhancement was present in 42 cases. Of these 28 were diffuse, 7 were peripheral around a poorly enhancing core, and 7 were a combination of different contrast enhancement patterns. Diffuse contrast enhancement was present in 6 of the 13 enlarged tendons.

Twenty three percent (n=10) of deep digital flexor tendinopathy cases (n=44) were visible at the level of the proximal interphalangeal joint, 64% (n=28) proximal to the navicular bone, 14 % (n=6) at the level of the navicular bone and 52 % (n=23) distal to the navicular bone (Fig. 2). Seventy one percent of the lesions were confined to one level and the most prevalent lesion level combination involved the level proximal to the navicular bone (50%, 39/78 possible lesion site combinations).

3.3. Distal interphalangeal osteoarthritis

Of the 37 extremities diagnosed with distal interphalangeal osteoarthritis (35%) (Fig. 3), 17 were grade 1, 17 grade 2 and 3 grade 3. Within grade 1, synovial distention and osteophyte formation, and minor cartilage defects were most frequent, whereas cartilage defects (n=14) were most frequent in grade 2 and 3 combined. Subchondral bone cyst formation (n= 3) was only present in grade 2-3. Synovial contrast enhancement was present in 3 grade 1 cases and 10 grade 2-3 cases. Joint narrowing was seen relatively infrequently (n=5) which may reflect the non-weightbearing of the examination (Table 1, supp Fig. 4).

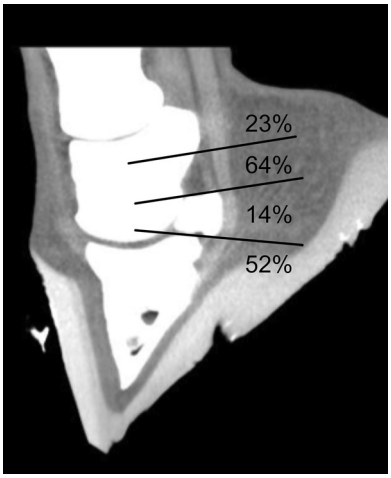

Fig. 2. Deep digital flexor tendon lesion zones: Percentages indicate the lesions at that level or which included that region as part of a larger lesion extending over multiple zones.

3.4. Navicular bursitis

Of the 32 extremities diagnosed with navicular bursitis (31%), 20 were grade 1, all of which had precontrast bursal distention. Adhesion formation or granulation tissue formation was present in seven cases. Synovial contrast enhancement was present in 14 cases (supp. Fig. 5). A concurrent diagnosis of navicular bone disease was present in 24 (75%) of cases and of deep digital flexor tendinopathy in 18 (56%).

3.5. Distal interphalangeal joint collateral ligament desmopathy

Of the 27 extremities diagnosed with distal interphalangeal joint collateral ligament desmopathy (26%), 18 were grade 1, with contrast enhancement (n=10) and insertional remodelling (n=7) most frequent. In combined grades 2 and 3 (n=9), enlargement and insertional remodelling was most frequent (supp. Fig. 6). In 15/27 (55%) of cases with distal interphalangeal joint collateral ligament desmopathy, a concurrent diagnosis of distal interphalangeal osteoarthritis was made, 12of 15 of which were grade 1 osteoarthritis.

3.6. Hoof capsule and distal phalanx pathology

There were 7 cases of keratoma (Fig. 4). Four cases of grade 1–2 of pedal osteitis and six cases of grade 1–2 abnormal laminae were also present.

3.7. Effect of weighting by conclusion and recommendation sections

A summary of diagnostic grading and diagnostic grading weighted by conclusion and recommendation sections is shown in Appendix 1. The results did not differ statistically ($P > .05$). This means that there was no difference between diagnoses made based on the findings section of the reports and diagnoses weighted by conclusion and recommendation section of the reports. The results of diagnoses weighted by conclusion and recommendation sections of the report are therefore not further separately described.

3.8. Result distribution after exclusion of all grade 1 lesions

The relative lesion distribution alters considerably when excluding all grade 1 cases, and combining all grade 2 and 3 cases for

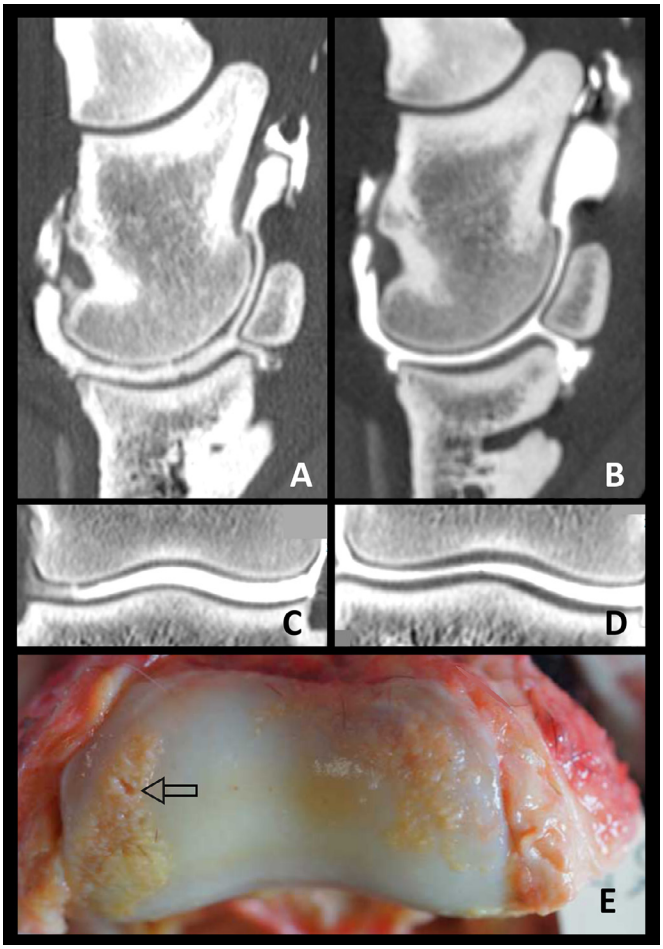

Fig. 3. (A), Sagittal multiplanar reconstruction of a distal interphalangeal CT arthrogram: Dorsal is to the left of the image. There is diffuse thinning of the articular cartilage with fibrillation of the cartilage evidenced by loss of margin outline and focal small full thickness defects of the articular surface evidenced by contrast agent contacting the subchondral bone plate. This is consistent with early osteoarthritis of the joint prior to other visible radiology findings. (B), Sagittal multiplanar reconstruction of the contralateral limb distal interphalangeal CT arthrogram. Image orientation, site and window and level settings are the same as for A: Dorsal is the left of the image. Normal cartilage outline is present. (C, D), Dorsal plane multiplanar reconstruction of a distal interphalangeal CT arthrogram of the affected and normal limb: Lateral is to the left of the image. Cartilage fibrillation and a full thickness defect is present on the lateral aspect of the image of the affected limb in comparison with the normal. (E), Postmortem gross image of the distal cartilage surface of the middle phalanx of the affected limb: Lateral is to the left of the image. Extensive cartilage fibrillation is present as well as a lateral focal full thickness cartilage defect (hollow arrow).

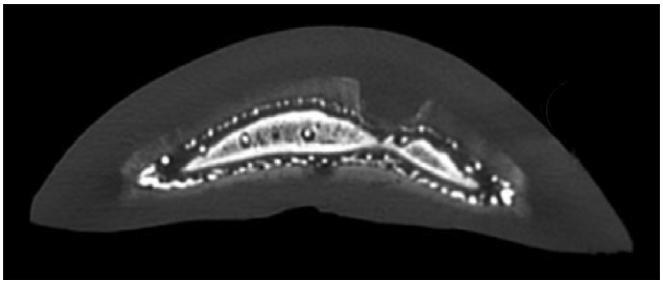

Fig. 4. Dorsal multiplanar reconstruction arteriogram at the level of the tip of the distal phalanx: There is focal complete loss of contrast enhancement within the vascular laminae and focal partial loss within the vasculature of the deep corium with focal resorption of the distal phalanx margin consistent with a keratoma of the cornified corium. Lateral is left on the image.

each main diagnostic group, effectively selecting only the diagnoses deemed likely or highly likely the cause of clinically significant lameness. Deep digital tendinopathy (n=36, or 34 % of total [N=105]) becomes the most frequent diagnosis, followed by distal interphalangeal osteoarthritis (n=20, 19% of total), navicular bone disease (n=18, 17% of total), navicular bursitis (n=12, 11% of total), hoof capsule and distal phalanx pathology (n=11, 10% of total), and collateral ligament desmopathy (n=9, 8% of total). This establishes a baseline prevalence of diagnoses considered clinically significant using this combination CT protocol.

4. Discussion

Deep digital tendinopathy, distal interphalangeal osteoarthritis, navicular bone disease, navicular bursitis, collateral ligament desmopathy, and hoof wall and distal phalanx pathology can be reliably, and with a biologically plausible range of severity diagnosed using this CT examination protocol.

The CT anatomy of the foot, the CT vascular anatomy, contrast CT normal images, comparative visualization and lesion conspicuity with low field MRI, and correlation between CT findings and macroscopic pathology has been described [3–5,7,10,12]. The current study is to the author's knowledge the first broad review of the CT examination findings of the equine distal extremities, and the first study combining the results of three contrast CT techniques. The results may provide an overview of the range, and severity of foot pathology detectable with CT and be a comparative point with other imaging modalities. The rationale for combining all contrast applications in the foot was to offset some of the disadvantages of CT imaging. Angiography allows for better visualization of intraparenchymal soft tissue lesions. Arthrography and bursography allows for good visualization of the outline of cartilage and synovial soft tissues. Pathology within the foot is often multiple and so all CT applications were combined to maximize diagnostic potential.

The population variables are representative of the standard clinic population presented for orthopaedic examination and of the countries' high percentage of thoroughbred horses used for sports and racing. Middle aged animals with a subacute to chronic mild to moderate lameness are consistent with the expected population referred for imaging.

Although duration of examination was not part of the current study, an average anaesthetic time of 1 and 1.5 hours is scheduled for a unilateral and bilateral four-stage foot CT examination respectively. The most time consuming aspects of the examination were the positioning of the horse and the ultrasound guided catheterization of the radial artery. The proximal placement of the catheter allows for contrast to be injected proximal to the bifurcation of the median palmar artery proximal to the metacarpophalangeal joint into the lateral and medial digital arteries. This would allow for a simultaneous lateromedial perfusion of the foot without streaking. In the later stages of the review, the distal interphalangeal arthrogram was often combined with the bursogram. Distending both synovial structures simultaneously was felt not to interfere with the interpretation and a reduction of anaesthetic time was achieved. No communication between the distal interphalangeal joint and the bursa was seen in the cases in which arthrogram and bursogram were performed sequentially, even though 5.3 % communication has been documented[13]. This may be due to technique differences, or subtle communication may have been not detected.

4.1. Overall results

There are few retrospective studies describing the entire range of imaging findings within the equine foot. The main diagnostic

results of a clinical non blinded study of 240 standing MRI examinations of 120 horses (compared with the current study) reported lameness in 71% of the limbs (87%), navicular disease in 69% (64%), deep digital flexor tendinopathy in 43% (43%), distal interphalangeal osteoarthritis in 47% (35%) navicular bursal distention in 60% (31%), and collateral ligament desmopathy of the distal interphalangeal joint in 12% (26%) [14]. The slightly higher diagnostic frequency of distal interphalangeal osteoarthritis (47% in comparison with 35% in this study) using standing MRI may be due to the high sensitivity and relatively lower specificity. Although low field MRI can identify a wide range of articular lesions (i.e high sensitivity), it can be argued that some of these lesions would possess a lower diagnostic specificity unless the identified articular lesions are pathognomonic. Under this assumption, MRI images may demonstrate a wide range of articular changes some of which could be regarded as false positives, explaining the higher diagnostic frequency. The reverse could be argued for collateral ligament desmopathy. The lesser soft tissue resolution of CT may result in an overdiagnosis due to relative low specificity.

Another review of standing MRI examination of 79 horses reported navicular bone lesions in 78%, navicular bursitis in 57%, deep digital tendinopathies in 54%, effusion of the distal interphalangeal joint in 53%, and collateral ligament desmopathy of the distal interphalangeal joint in 39%. In the same study, 94% had alterations in more than one structure in the lame or lamest foot [15], which is consistent with our results. A recent review of 550 equine foot MRI examinations reported navicular bone abnormalities in 74%, distal interphalangeal joint abnormalities in 65% and deep digital flexor tendon abnormalities in 47% of cases[16]. Overall, the lesion distribution between the current study and findings from several standing MRI retrospective studies overlap.

4.2. Navicular bone disease

In the current study, the relative low number of cases with likely or definitively clinically relevant disease (grade 2 and 3) is expected. Many of the more severe changes would likely have been radiographically visible, therefore reducing the need for referral for imaging. This introduces a selection bias against cases with moderate or severe navicular bone disease. The very low rate of distal sesamoidean ligament and collateral sesamoidean ligament imaging findings is likely due to the low conspicuity of these ligaments in CT or CTA. This is comparable to the low conspicuity of the distal sesamoidean ligaments of the fetlock found with contrast CT[17]. Contrast in the distal interphalangeal joint was still clearly present during the bursography phase. The collateral sesamoidean and distal sesmoidean ligament were therefore clearly outlined on both sides by contrast in the bursography phase. Despite the increased visibility of the margins, few shape changes were seen in those ligaments.

Unlike MRI, CT does not have the capacity to visualize an increased fluid signal in the navicular bone, and will therefore fail to detect navicular disease cases in which there is only increased fluid signal within the bone and no bony morphological changes. CT will also not demonstrate increased fluid in the trabecular bone of other bones of the distal limb such as occurs in the dorsal distal second phalanx if these lesions are not associated with bony changes. An increased fluid signal on STIR FSE MRI images within the trabecular bone may reflect oedema, haemorrhage, necrosis, degeneration or physiologic stress remodeling [18]. Degenerative injury of the navicular bone is therefore indistinguishable from contusion or physiologic stress remodelling of the navicular bone when there is no compact or trabecular bone damage [16]. An increased trabecular bone fluid signal has also shown to be prevalent in non-symptomatic horses [19]. Higher grade STIR FSE fluid signal in the navicular bone are associated with other morphological changes [18], therefore it may be reasonable to suggest that navicular bone alterations over and above physiologic stress remodelling or oedema may be diagnosed with CT based on the morphologic changes to the bone. Increased fluid within the bone may be in the future visible using dual-energy CT. In human medicine promising results have been published for dual energy CT to detect bone marrow oedema [20,21].

In the current study, the navicular bursogram provided consistently good visualization of the flexor fibrocartilage of the navicular bone. Thinning of the cartilage or full thickness erosions were clearly visible, and these imaging findings contributed to the navicular disease diagnosis score. Using a CT scout image to confirm needle placement was very quick and reliable, which is why this approach was followed. A disadvantage of this approach is the morbidity of puncturing the deep digital flexor tendon. A ultrasound guided tendon sparing approach may be an alternative [22,23].

4.3. Navicular bursitis

In a low field MRI and high field MRI review, navicular bursitis was present in 57% of cases and bursal effusion in 49% of cases respectively [14,24], which is higher than the 26% in this review. This may be due to lower conspicuity of the fluid in the pre-contrast CT images, or due to a higher threshold to report increased filling of the bursa by the authors of this study. Relatively few adhesions were visualized in cases of navicular bursitis in this study. Of 26 cases in which bursal adhesions were suspected using high field MRI, only 19 were positively diagnosed to have one or more adhesions [25]. In that study, a positive predictive value for the presence of adhesions was 50% for loss of separation between the deep digital flexor tendon and bursa or collateral sesamoidean ligament, 67% for focal disruption of the signal of bursa fluid with presence of abnormal tissue and 100% for well-defined abnormal tissue was seen between the two structures [25]. It is reasonable to consider that bursal distention and presence of contrast agent in CT bursography would increase adhesion conspicuity, and therefore reduce false positives. This may give support to the observation from this study that adhesion formation is an infrequent occurrence and supports the use of a bursogram. In the current study, navicular bursa findings of grade 2–3 were often in association with higher grade findings (56%) of the navicular apparatus or deep digital flexor tendon. Using high field MRI, of 16 cases with positively confirmed bursal adhesions, 94% had bursal effusion, 81% had deep digital flexor tendon abnormalities, 94% had navicular bone abnormalities, 56% has collateral sesamoidean ligament abnormalities and 50% had impar ligament abnormalities [25]. This corresponds with the findings of the current study that higher grade bursal abnormalities are generally associated with higher grade pathology in the navicular bone and deep digital flexor tendon (Fig. 5).

An observation during the bursography phase was that during injection often a lower volume of contrast was required and higher back pressure on the syringe was felt in cases of severe navicular bursitis. A possible explanation is fibrosis of the bursal synovium and capsule, reducing joint capsule compliance. Contrast was still present in the distal interphalangeal joint in the cases in which the arthrography and bursography was performed sequentially. This did not interfere with interpretation, nor did it interfere in cases in which arthrography and bursography was performed simultaneously.

4.4. Deep digital flexor tendinopathy

A relatively large proportion of clinically significant deep digital flexor tendon lesions would be expected in a lame population with little radiographically visible abnormalities. Most of the horses in

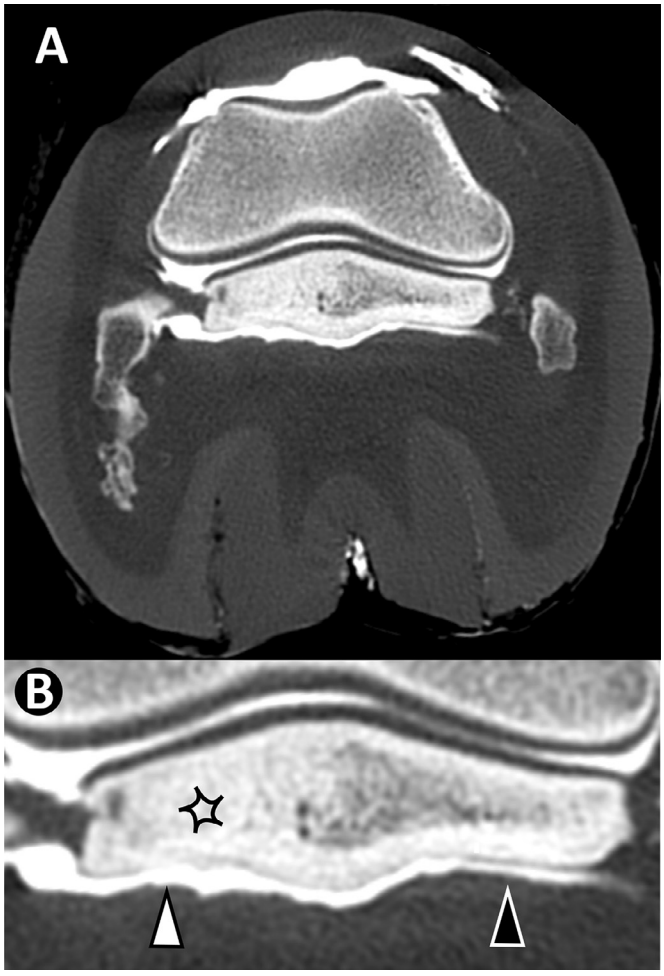

Fig. 5. Transverse multiplanar reconstruction distal interphalangeal arthrogram and bursogram and at the level of the navicular bone: Lateral is to the left of the image. There is complete loss of fibrocartilage at the lateral flexor cortex with contrast agent in contact with the bone (WHITE ARROWHEAD), and partial loss at the medial aspect (BLACK ARROWHEAD). In addition there is focal navicular bone medullary sclerosis (HOLLOW STAR) and an irregular dorsal border to the deep digital flexor tendon, worse laterally than medially. The dorsal articular cartilage of the navicular bone is intact.

the current study would have had one or more radiographic foot examinations prior to referral. The preponderance of grade 2–3 deep digital flexor tendon lesions is therefore expected considering the selection bias reported above. Deep digital flexor tendon lesions identified by intra-arterial contrast-enhanced CT have a high true positive (93%) and true negative (88%) detection rate compared with macroscopic examination [7].

The relatively low number of deep digital flexor tendon splits diagnosed (n=2) is unexpected as contrast agent would be expected to dissect between the fibre bundles in the region adjacent to the navicular bursa in the bursography phase. The authors hypothesize that the presence of an intact epitenon or granulation tissue covering splits within the tendon parenchyma may have reduced the visibility of the splits during the bursography phase. In another study, the majority of deep digital flexor tendinopathy cases diagnosed by non-contrast enhanced CT were core lesion (96%) and dorsal border irregularities (73%) [26].

The low percentage (14%) of lesions at the level of the navicular bone detected in the current study reflects the difficulty of CT to diagnose deep digital flexor tendon lesions in the region of the navicular bone and therefore tendinopathy in that region is likely underdiagnosed [7,10]. In the current study, a great percentage (64%) of the lesions involved the suprasesamoidean region. In a review of 264 cases using high field MRI, lesions at the level of the proximal interphalangeal joint were present in 29%, at the level of the collateral sesamoidean ligaments in 59%, at the level of the navicular bone in 59%, at the distal sesamoidean ligament in 35 % and at the deep digital flexor tendon insertion in 37% respectively [24].

Some distinctive patterns of contrast enhancement of the deep digital flexor tendon were present. Peripheral contrast enhancement around a hypoattenuating core likely represents focal avascular necrosis with peripheral angiogenesis. Fine diffuse increased contrast enhancement of the tendon likely represents a diffuse tendinopathy with increased flow of existing microvasculature or angiogenesis associated with an active inflammatory or degenerative response. This pattern was seen in enlarged as well as normal sized tendon lobes. Diffuse contrast enhancement at the dorsal aspect of the tendon may be associated with dorsal border fibrillation and/or fibrocartilaginous metaplasia not visible on native soft tissue algorithm CT. Macroscopic histologic correlation of some of these findings is available [7], but further histologic correlation is required to support these interpretations.

4.5. Distal interphalangeal osteoarthritis

One of the earliest pathological changes in the onset of osteoarthritis is cartilage degeneration [27]. Positive contrast CT arthrography increases the conspicuity of small cartilage lesions and therefore of early joint degeneration. Mean sensitivity for localizing cartilage defects in the equine carpus in a blinded experimental study concluded CT arthrography showing the best sensitivity (69.9%), followed by high field magnetic resonance arthrography (53.5%), high field MRI (33.3%), and CT (18.1%) respectively [9]. Low field MRI was not included in the comparison. The higher percentage of grade 1 lesions in the current study is expected as more advanced osteoarthrosis would likely be more visible radiographically, reducing the likelihood of referral for CT examination. The ability to visualize early cartilage pathology using this protocol may be clinically relevant. The authors found that focal as well as diffuse partial thickness lesions of the articular cartilage were easy to discern. In the few cases for which postmortem findings were available, the imaging findings still underestimated the macroscopic findings (Fig. 3). The CT arthrogram combined with the high sensitivity of native bone algorithm CT to visualize subchondral bone plate sclerosis was felt to be very useful to diagnose early osteoarthritic changes.

Approximately 55% of horses diagnosed with collateral ligament desmopathy in this study had concurrent distal interphalangeal osteoarthritis. This is also expected considering the close association with the joint. The collateral ligament is difficult to discern on native soft tissue algorithm CT. A CT angiogram did generally not enhance conspicuity of the margins of an assumed normal collateral ligament. In some cases, there was focal vascular enhancement, generally at the insertion or origin, interpreted as vascular dilation or neovascularization secondary to pathology. Synovial contrast is often visible in the distal interphalangeal synovial pouches axial and sometimes caudal to the insertion of a normal collateral ligament during the distal interphalangeal arthrogram, and is considered normal. In some cases, synovial contrast agent was seen within the insertion of the collateral ligament, and interpreted as tearing of the insertion. Combined with the ability of native bone algorithm CT to visualize bony origin and insertional remodeling, this was perceived to compensate for some of the poor soft tissue resolution of native soft tissue algorithm CT to diagnose collateral ligament desmopathy.

4.6. Hoof capsule and distal phalanx pathology

Seven keratoma which were unknown prior to examination were diagnosed, of which five were grade 2–3. Keratoma are relatively easy to diagnose using CT and CT has been used effectively for pre-operative planning [28,29]. Of the four cases with pedal osteitis, 2 were grade 2. The diagnosis was mainly based on the description of circumferential lysis of the distal phalanx solar margin.

4.7. Limitations

The findings of this review are relevant to the referral population included in this study.

Descriptive statistics only were used and no inference to lameness is made. Diagnoses were based on imaging findings only from the radiology reports. The severity grading of these findings was subjective. Given that a pre-determined grading scheme was not used, repeatability of the review is limited. The review is also based on imaging reports from two qualified but unblinded readers. The distribution and weighting of imaging findings in the reports may also have evolved over time. The result that there was no clinically significant difference between grading based on the findings section of the report and grading with weighting based on the conclusion and recommendation section of the report is expected as the grading, even though based on objective criteria, is a subjective process itself. The comparison was made only to see if there is consistency between findings and conclusions in the radiology reports. No inference to histologic abnormalities is made in the study.

It could be argued that an abaxial nerve block as inclusion criterium is not selective enough as metacarpophalangeal pain can be abolished in some horses. For that reason, horses with positive findings in the included metacarpophalangeal region in the native image series were excluded from the review, reducing the possible confounding influence.

A concentration of 150 mgL/mL of iodinated contrast agent was used for the arthrogram and bursogram phase. A lower concentration of 35–40 mgL/mL is reported to induce less blooming artifact [6,30] [31], whereas other studies report satisfactory results using a higher 100–150 mgL/mL concentration [8] [32]. The authors did not experience limitations in assessing the synovial surfaces, but did require to window/level the images during interpretation. The higher concentration of contrast agent was maintained throughout the study for consistency. Correlating diagnostic grade, and a combination of imaging findings with lameness and laterality may be useful and could be considered in the future.

4.8. Conclusions

In conclusion, navicular bone changes were the most prevalent diagnostic category of which only one quarter were deemed clinically significant. Deep digital flexor tendon lesions were found in half of the limbs, of which the great majority were considered clinically significant. Distal interphalangeal joint pathology was found in one third of examined limbs of which half were considered clinically significant. Navicular bursa and collateral ligament abnormalities were found in a quarter of all examined limbs, of which one third of each were clinically significant. Navicular bursa abnormalities were associated with navicular bone and deep digital flexor tendon lesions. By performing three contrast applications per foot, a maximum amount of information was efficiently obtained. The results of this study demonstrate that a range of findings with a varied severity and a broad range of diagnoses can be established using this combined CT protocol; and that the range of diagnoses is comparable to those obtained by other cross-sectional imaging modalities.

Acknowledgments

The authors are very grateful to the horse owners, referring veterinarians, Equine Hospital clinicians, and imaging technicians without whom this would not have been possible. The authors are also very grateful for the expert processing and composition of the illustrations by Professor Joe Mayhew.

Authors' contributions

FP contributed to conceptualization, methodology, formal analysis, investigation, resources, writing, reviewing, editing and final editing, visualization, supervision and project administration. AH contributed to conceptualization, formal analysis, reviewing and editing. JAA contributed to methodology, formal analysis, reviewing, editing and visualization. PW contributed to resources, reviewing, supervision and project administration. JS contributed to conceptualization, methodology, reviewing, editing, and supervision.

Financial disclosure

This research did not receive any specific grant from funding agencies in the public, commercial, or not-for-profit sectors.

Supplementary materials

Supplementary material associated with this article can be found, in the online version, at doi:10.1016/j.jevs.2021.103704.

Appendix 1

	Diagnostic Grading			Diagnostic Grading Weighted By Clinical Significance			
	Mean (SD)	Median(Q1, Q3)	Min, Max	Mean (SD)	Median(Q1, Q3)	Min, Max	*P* value*
Ddft core lesion	0.74 (1)	0 (0, 2)	0, 3	0.86 (1.14)	0 (0, 2)	0, 3	.6
Ddft split lesion	0.05 (0.35)	0 (0, 0)	0, 3	0.05 (0.35)	0 (0, 0)	0, 3	1
Ddft dorsal border lesion	0.36 (0.67)	0 (0, 1)	0, 2	0.40 (0.74)	0 (0, 1)	0, 3	.89
Navicular bursitis	0.44 (0.75)	0 (0, 1)	0, 3	0.49 (0.86)	0 (0, 1)	0, 3	.91
Navicular bone disease	0.82 (0.73)	1 (0, 1)	0, 3	0.90 (0.86)	1 (0, 1)	0, 3	.69
Impar ligament desmopathy	0.15 (0.50)	0 (0, 0)	0, 3	0.15 (0.48)	0 (0, 0)	0, 2	.99
CSL desmopathy	0.06 (0.33)	0 (0, 0)	0, 2	0.06 (0.33)	0 (0, 0)	0, 2	1
DIPJ Colateral Ligament desmopathy	0.36 (0.70)	0 (0, 1)	0, 3	0.40 (0.78)	0 (0, 1)	0, 3	.91
DIPJ osteoarthritis	0.57 (0.86)	0 (0, 1)	0, 3	0.67 (1.02)	0 (0, 1)	0, 3	.92
Laminar contrast abnormal	0.08 (0.33)	0 (0, 0)	0, 2	0.09 (0.40)	0 (0, 0)	0, 3	.99
Keratoma	0.13 (0.54)	0 (0, 0)	0, 3	0.16 (0.62)	0 (0, 0)	0, 3	.99
Pedal osteitis	0.06 (0.30)	0 (0, 0)	0, 2	0.06 (0.30)	0 (0, 0)	0, 2	.99

Wilcoxon rank sum test with continuity correction *P* values

References

[1] Porter EG, Werpy NM. New concepts in standing advanced diagnostic equine imaging. Vet Clin North Am-Equine Pract. 2014;30(1):239–67.

[2] d'Anjou M-A. Principles of computed tomography and magnetic resonance imaging. In: Thrall DE, ed. *Textbook of Veterinary Diagnostic Radiology.*Philadelphia, United States: Elsevier; 2012:50-73.

[3] Vallance SA, Bell RJW, Spriet M, Kass PH, Puchalski SM. Comparisons of computed tomography, contrast enhanced computed tomography and standing low-field magnetic resonance imaging in horses with lameness localized to the foot. Part 1: anatomic visualization scores. Equine Vet J. 2012;44(1):51–6.

[4] Puchalski SM, Galuppo LD, Hornof WJ, Wisner ER. Intraarterial contrast-enhanced computed tomography of the equine distal extremity. Vet Radiol Ultrasound. 2007;48(1):21–9.

[5] Collins JN, Galuppo LD, Thomas HL, Wisner ER, Hornof WJ. Use of computed tomography angiography to evaluate the vascular anatomy of the distal portion of the forelimb of horses. Am J Vet Res. 2004;65(10):1409–20.

[6] Nelson BB, Goodrich LR, Barrett MF, Grinstaff MW, Kawcak CE. Use of contrast media in computed tomography and magnetic resonance imaging in horses: techniques, adverse events and opportunities. Equine Vet J. 2017;49(4):410–24.

[7] van Hamel SE, Bergman HJ, Puchalski SM, de Groot MW, van Weeren PR. Contrast-enhanced computed tomographic evaluation of the deep digital flexor tendon in the equine foot compared to macroscopic and histological findings in 23 limbs. Equine Vet J. 2014;46(3):300–5.

[8] Gray SN, Puchalski SM, Galuppo LD. Computed tomographic arthrography of the intercarpal ligaments of the equine carpus. Vet Radiol Ultrasound. 2013;54(3):245–52.

[9] Sanchez-Andrade JS, Richter H, Kuhn K, Bischofberger AS, Kircher PR, Hoey S. Comparison between magnetic resonance imaging, computed tomography, and arthrography to identify artificially induced cartilage defects of the equine carpal joints. Vet Radiol Ultrasound. 2018;59(3):312–25.

[10] Vallance SA, Bell RJW, Spriet M, Kass PH, Puchalski SM. Comparisons of computed tomography, contrast-enhanced computed tomography and standing low-field magnetic resonance imaging in horses with lameness localized to the foot. Part 2: lesion identification. Equine Vet J. 2012;44(2):149–56.

[11] Moyer W, Schumacher J, Schumacher J. Equine Joint Injection and Regional Anesthesia. Academic Veterinary Solutions, LLC; 2011.

[12] Claerhoudt S, Bergman EHJ, Saunders JH. Computed tomographic anatomy of the equine foot. Anat Histol Embryol 2014;43(5):395–402.

[13] Hontoir F, Rejas E, Falticeanu A, et al. Communication between the distal interphalangeal joint and the navicular bursa in the horse at Computed Tomography Arthrography. Anat Histol Embryol. 2019;48(2):133–41.

[14] Stockl T, Schulze T, Brehm W, Gerlach K. Comparative bilateral magnetic resonance imaging of the foot in low-field MRI - Part 1: findings and development of a grading system. Pferdeheilkunde 2013;29(2):191–201.

[15] Gutierrez-Nibeyro SD, Werpy NM, White NA. Standing low-field magnetic resonance imaging in horses with chronic foot pain. Aust Vet J 2012;90(3):75–83.

[16] Gutierrez-Nibeyro SD, Werpy NM, Gold SJ, Olguin S, Schaeffer DJ. Standing MRI lesions of the distal interphalangeal joint and podotrochlear apparatus occur with a high frequency in warmblood horses. Vet Radiol Ultrasound 2020;61(3):336–45.

[17] Rasmussen L, Saunders JH, Van der veen H, Raes E, Van veggel E, Vanderperren K. Contrast-enhanced computed tomography features of oblique and straight distal sesamoidean ligament injury in thirty-one horses. Vlaams Diergeneeskundig Tijdschrift 2018;87(5):245–54.

[18] Dyson S, Blunden T, Murray R. Comparison between magnetic resonance imaging and histological findings in the navicular bone of horses with foot pain. Equine Vet J. 2012;44(6):692–8.

[19] De Guio C, Segard-Weisse E, Thomas-Cancian A, Schramme M. Bone marrow lesions of the distal condyles of the third metacarpal bone are common and not always related to lameness in sports and pleasure horses. Vet Radiol Ultrasound 2019;60(2):167–75.

[20] Suh CH, Yun SJ, Jin W, Lee SH, Park SY, Ryu CW. Diagnostic performance of dual-energy CT for the detection of bone marrow oedema: a systematic review and meta-analysis. Eur Radiol 2018;28(10):4182–94.

[21] Diekhoff T, Engelhard N, Fuchs M, et al. Single-source dual-energy computed tomography for the assessment of bone marrow oedema in vertebral compression fractures: a prospective diagnostic accuracy study. Eur Radiol. 2019;29(1):31–9.

[22] Nottrott K, De Guio C, Khairoun A, Schramme M. An ultrasound-guided, tendon-sparing, lateral approach to injection of the navicular bursa. Equine Vet J. 2017;49(5):655–61.

[23] Estrada RJ, Pascual A, Lischer CJ. Development and Evaluation of Ultrasound-Guided Navicular Bursa Injection Using the Palmarodistal Digital Approach in Horses: an Ex Vivo Study. J Equine Vet Sci 2015;35(10):849–55.

[24] Dyson S, Murray R. Magnetic resonance imaging evaluation of 264 horses with foot pain: The podotrochlear apparatus, deep digital flexor tendon and collateral ligaments of the distal interphalangeal joint. Equine Vet J 2007;39(4):340–3.

[25] Holowinski ME, Solano M, Maranda L, Garcia-Lopez JM. Magnetic resonance imaging of navicular bursa adhesions. Vet Radiol Ultrasound. 2012;53(5):566–72.

[26] Jones ARE, Ragle CA, Mattoon JS, Sanz MG. Use of non-contrast-enhanced computed tomography to identify deep digital flexor tendinopathy in horses with lameness: 28 cases (2014-2016). J Am Vet Med Assoc 2019;254(7):852–8.

[27] Kawcak CE. 4 - Pathologic manifestations of joint disease. In: McIlwraith CW, Frisbie DD, Kawcak CE, van Weeren PR, eds. *Joint Disease in the Horse (Second Edition).*Edinburgh: W.B. Saunders; 2016:49-56.

[28] Getman LM, Davidson EJ, Ross MW, Leitch M, Richardson DW. Computed tomography or magnetic resonance imaging-assisted partial hoof wall resection for keratoma removal. Vet Surg 2011;40(6):708–14.

[29] Katzman SA, Spriet M, Galuppo LD. Outcome following computed tomographic imaging and subsequent surgical removal of keratomas in equids: 32 cases (2005–2016). J Am Vet Med Assoc 2019;254(2):266–74.

[30] Vanderperren K, Ghaye B, Snaps FR, Saunders JH. Evaluation of computed tomographic anatomy of the equine metacarpophalangeal joint. Am J Vet Res 2008;69(5):631–8.

[31] Gendler A, Keuler NS, Schaefer SL. Computed tomographic arthrography of the normal canine elbow. Vet Radiol Ultrasound 2015;56(2):144–52.

[32] Bergman EHJ, Puchalski SM, van der Veen H, Wiemer P. Computed tomography and computed tomography arthrography of the equine stifle: technique and preliminary results in 16 clinical cases. Paper presented at: AAEP Annual Convention- Orlando; 2007.